Journal of Alloys and Compounds, 194 (1993) 13–17
JALCOM 460

Crystal structure and magnetic properties of $D_uY_2BaCuO_5$ ($u=0.00$, 0.61, 1.31)

H. Shaked
Nuclear Research Center-Negev, P.O.B. 9001, Beer Sheva (Israel) and Ben Gurion University of the Negev, P.O.B. 653, Beer Sheva (Israel)

H. Pinto, H. Ettedgui, Z. Gavra and M. Melamud
Nuclear Research Center-Negev, P.O.B. 9001, Beer Sheva (Israel)

J. R. Johnson and J. J. Reilly
Department of Applied Science, Brookhaven National Laboratory, Upton, NY 11973 (USA)

(Received August 3, 1992)

Abstract

Samples of $D_uY_2BaCuO_5$ ($u=0.61$, 1.31), were prepared by a direct reaction of the green phase (Y_2BaCuO_5) with D_2 gas. The crystallographic structure of the three compounds ($u=0.00$, 0.61, 1.31) were studied using X-ray and neutron powder diffraction. It was found that as D enters the green phase, a solid solution phase is formed with no symmetry change. Two sites partially occupied by D were determined. The occupancy of these sites is consistent with a maximum solubility of $u=2$. The temperature dependence of the magnetic susceptibility of the three samples obeyed the Curie–Weiss law with antiferromagnetic interaction. The paramagnetic Curie temperature decreased with deuteriding, while, the Cu^{++} magnetic moment remained unchanged.

1. Introduction

The oxide Y_2BaCuO_5 was discovered [1] in 1982. Five years later it became to be known as the "green phase", which appeared [2, 3] as a second phase in some preparations of the high T_c oxide superconductor $YBa_2Cu_3O_7$. Its crystallographic structure was studied by powder X-ray diffraction [1, 4], single crystal X-ray diffraction [5], and powder neutron diffraction [6]. It was found to have an orthorhombic structure belonging to the space-group [7] *Pnma* (No. 62). It has a large unit cell, with the dimensions: $12.2\times5.65\times7.13$ Å^3, which contains four formula units.

An onset to antiferromagnetic order at $T_N=13$–15 K was discovered in electron paramagnetic resonance (EPR) [8, 9], magnetic susceptibility [9], muon-spin rotation (μ^+SR) [10] and specific heat [11, 12] studies of this oxide.

The green phase had been found to react directly with H_2 gas to form the crystalline addition compound $H_uY_2BaCuO_5$ [13]. It was found that a solid solution phase was formed without structural change for uptakes up to $u=2$. As u was increased a second H-rich phase emerged and it was possible to increase u to a maximal value of 3.9 [13]. The lattice expansion due to hydriding is small, and the fractional molar volume was found to be smaller than 1 Å^3 (H atom)$^{-1}$. Similar fractional molar volumes were also reported [14] for the hydriding of the oxide $YBa_2Cu_3O_7$. This is small compared to the fractional molar volumes of approximately 2.9 Å^3 (H atom)$^{-1}$ found [15, 16] in most metals hydrides. Hence, it is reasonable to expect that large interstices are the hosts of hydrogen atoms in these oxides.

In the present paper we report the results of the following studies of $D_uY_2BaCuO_5$ with $u=0.00$, 0.61, 1.31. (Deuterium was used in these samples instead of hydrogen, in order to avoid the high background resulting from the anomalously high incoherent neutron scattering amplitude of H.) (i) Site positions of D, using neutron powder diffraction; (ii) paramagnetic constants, using a.c. magnetic susceptibility.

2. Experimental details, analysis, and results

The procedure for the preparation of the starting oxide Y_2BaCuO_5 was reported previously [13]. The deuterium compounds were prepared by the direct reaction of the (non-platinized) oxides with D_2 gas. The deuteriding procedure for the oxides was as follows:

0925-8388/93/$6.00

a sample of approximately 20 gr (−100 mesh) was introduced into a stainless steel reactor of a known volume and out-gassed at 393 K for a period of 30 min. At the end of this period the out-gassed sample was cooled to room temperature, then, D_2 gas was introduced into the reactor to give a pressure of 50–55 atm. The reactor was then heated to 398–473 K, and the deuteriding began immediately. The colour of the oxide turned from green to brown-black upon deuteriding. The deuteriding took several weeks to a couple of months to complete, depending on the desired content of the final deuteride. Heating the starting oxide above 473 K leads to its reduction, and was therefore avoided. The sample uptake of D_2 was followed by recording the gas pressure as a function of time. The deuterium content of the final deuterides was calculated from the overall decrease of the D_2 pressure at room temperature. Two samples of $D_uY_2BaCuO_5$ of approximately 20 gr were prepared according to this procedure. The final u values (as determined from the D_2 pressure decrease) of the two samples were 0.61 and 1.31.

X-ray ($\lambda = 1.5418$ Å) diffraction patterns of powder samples of $D_uY_2BaCuO_5$ with $u = 0.00$, 0.61, 1.31, which were taken from the three preparations, are shown in Fig. 1. No lines other than those of Y_2BaCuO_5 are observed in the pattern of the starting material ($u = 0.00$). The X-ray patterns of the deuterided samples (Fig. 1, center and top) show no lines other than those of the nondeuterided sample (bottom). A definite increase of line width and background is observed in these patterns with deuteriding.

Neutron ($\lambda = 2.403$ Å) diffraction patterns of the powder samples of $D_uY_2BaCuO_5$ with $u = 0.00$, 0.61, 1.31, are shown in Fig. 2. The neutron patterns exhibit

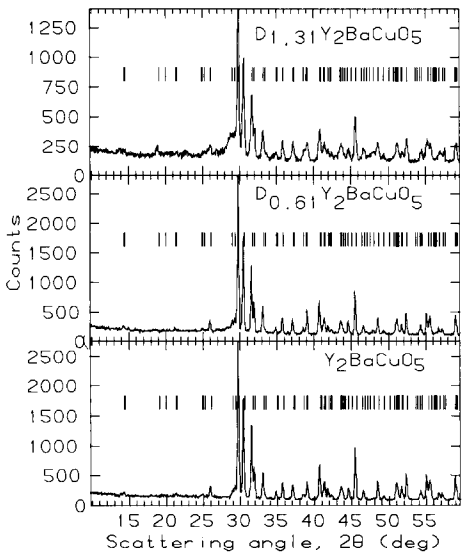

Fig. 1. X-ray (Cu K_α) diffraction of $D_uY_2BaCuO_5$ with $u = 0.00$ (bottom), 0.61 (center), 1.31 (top).

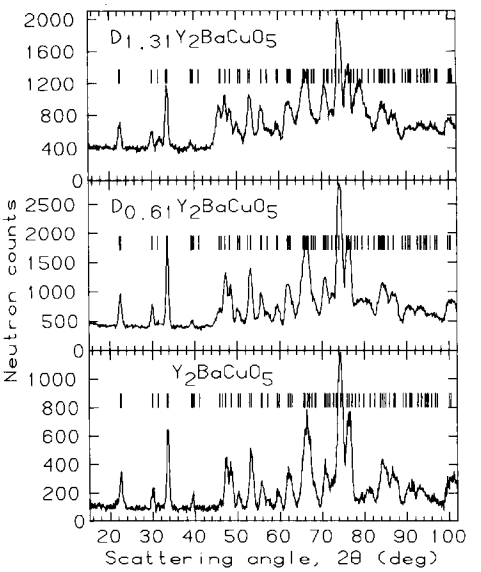

Fig. 2. Neutron ($\lambda = 2.403$ Å) diffraction of $D_uY_2BaCuO_5$ with $u = 0.00$ (bottom), 0.61 (center), 1.31 (top).

essentially the same features observed in the X-ray patterns, namely: (i) no lines other than those of the non-deuterided oxide; (ii) an increase of line width and background with deuteriding.

Unlike X-rays, the neutron patterns exhibit marked changes in the relative intensity of some lines (*e.g.* $2\theta = 46$, 79). Another apparent difference is the shape of the background, namely, the X-rays form a "flat" background, whereas, the neutron background tends to form a broad hump in the $2\theta \approx 50$–$90°$ region. A neutron diffraction pattern of the sample with $u = 1.31$, taken (not shown) with the sample at a temperature of 10 K, is essentially identical to the one taken at room temperature (Fig. 2, top). This result shows that the hump in the background is not due to thermal diffuse scattering.

The Wiles and Young least squares (Rietveld) analysis [17, 18], modified for neutron diffraction [19], was used to analyse each one of the three neutron diffraction patterns. In this analysis the structural parameters of the sample are refined so that the calculated pattern will best fit (least squares) the observed pattern. The orthorhombic symmetry, with space-group [7] *Pnma*, was used in the analysis of the three samples. A typical refinement included 82 reflections and 30–36 variable parameters. A summary of the results of the refinements is given in Table 1. The background function in this analysis is a polynomial of the fifth degree in 2θ. The refined coefficients of the polynomials (not listed in the table) yielded background functions with a broad hump in the region $2\theta \approx 50$–$90°$ for the $u = 0.61$ and 1.31 patterns. Due to the low values of $\sin\theta/\lambda$ (< 0.31), the dependence of the fit on the refined Debye–Waller factors (B), is very weak. This led to a poor convergence

TABLE 1. Structural parameters for $D_uY_2BaCuO_5$ with $u=0.00$, 0.61, 1.31. Rietveld refinements were done in the orthorhombic space-group: *Pnma*. The atom positions are: Y(1)(x, 1/4, z), Y(2)(x, 1/4, z), Ba(x, 1/4, z), Cu(x, 0.25, z), O(1)(x, y, z), O(2)(x, y, z), O(3)(x, 1/4, z), D(1)(x, y, z), D(2)(x, y, z). The following isotropic Debye–Waller factors were used: B(Y)=0.2, B(Ba)=0.15, B(Cu)=0.25, B(O)=0.45, B(D)=0.7. The weighted agreement factor, R_w, and the expected agreement factor, R_{exp}, are given in the last two lines [18]. Numbers in parentheses are statistical errors of the last significant digits

		u		
		0.00	0.61	1.31
a (Å)		12.180 (4)	12.184 (4)	12.192 (7)
b (Å)		5.654 (2)	5.655 (2)	5.653 (3)
c (Å)		7.135 (3)	7.130 (2)	7.156 (4)
V (Å^3)		491.3 (3)	491.2 (3)	493.2 (5)
Y(1):	x	0.2886 (6)	0.2872 (8)	0.2913 (17)
	z	0.1155 (15)	0.1268 (19)	0.1089 (28)
Y(2):	x	0.0721 (8)	0.0747 (13)	0.0834 (16)
	z	0.3965 (9)	0.3984 (18)	0.3866 (32)
Ba:	x	0.9014 (10)	0.9029 (16)	0.9110 (22)
	z	0.9324 (19)	0.9434 (25)	0.9770 (32)
Cu:	x	0.6583 (9)	0.6714 (15)	0.6298 (16)
	z	0.7132 (12)	0.7060 (15)	0.6965 (24)
O(1):	x	0.4349 (7)	0.4294 (10)	0.4224 (18)
	y	0.5071 (14)	0.5364 (17)	0.4855 (24)
	z	0.1645 (7)	0.1698 (10)	0.1940 (26)
O(2):	x	0.2268 (7)	0.2289 (8)	0.2071 (11)
	y	0.5067 (19)	0.4807 (26)	0.5603 (31)
	z	0.3518 (13)	0.3543 (17)	0.2983 (31)
O(3):	x	0.0978 (11)	0.0988 (16)	0.0998 (25)
	z	0.0754 (16)	0.0755 (26)	0.0718 (34)
D(1):	x	–	0.5037 (50)	0.5241 (34)
	y	–	0.0698 (87)	0.0285(104)
	z	–	0.1079 (66)	0.0214 (85)
	u	–	0.4323(143)	0.8386(102)
D(2):	x	–	0.0131 (86)	0.0278 (80)
	y	–	0.6412(163)	0.4837(122)
	z	–	0.0929(150)	0.9868(131)
	u	–	0.1777(143)	0.4714(102)
R_w (%)		12.58	14.60	23.36
R_{exp} (%)		7.55	8.36	10.65

of the analysis whenever the B's were set as variable parameters. Hence, the B's were fixed at the values given in Table 1. Moderate changes in these values have little effect on the refined values of the other parameters. Two non-equivalent (general position) sites for the deuterium, were used in the refinement of the crystallographic structure. The refined positions of the two sites pair up near two inversion centers: D(1) at 1/2 0 0, and D(2) at 0 1/2 0. Refinements with a single (general position) site, converged poorly and haphazardly near one of the two centers, yielding values of R_w 3–5% higher than those listed in Table 1.

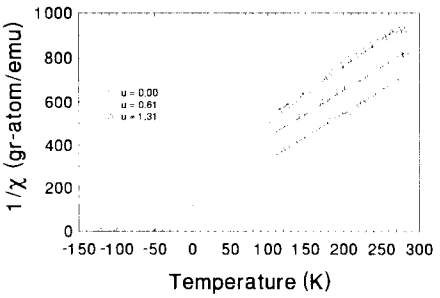

Fig. 3. The temperature dependence of the inverse magnetic susceptibility of $D_uY_2BaCuO_5$ ($u=0.00$, 0.61, 1.31). Straight (dashed) lines correspond to Curie–Weiss law, using the best fit constants of Table 2.

Magnetic a.c. susceptibilities were measured as a function of temperature, in the temperature range $T=80$–300 K, for small samples taken from the three preparations. The measurement apparatus consisted of a primary (exciting) coil coaxial with a pair of balanced secondary (detection) coils. The sample was mounted, in contact with a thermocouple junction, at the end of a coaxial travelling glass rod, which moved the sample from the center of one secondary coil to the center of the other. The sample travelling period between coils was 7 s, during which the sample was stationary for 0.30 s, 0.15 s at the center of each coil. The off-balance voltage induced in the secondary coils, and the thermocouple voltage were recorded for the 0.15 s intervals during which, the sample is stationary at the coil centers. A sinusoidal exciting current, with a rms value of 10 mA and a frequency of 1105 Hz, was driven through the primary coil. The corresponding rms value of the a.c. magnetic field at the sample is (calculated) approximately 1.2 Oe. The instrument was calibrated using the paramagnetic oxides Gd_2O_3, Dy_2O_3, Ho_2O_3, and Er_2O_3, and it was found that the off balance voltage was proportional to the published magnetic susceptibility with a factor of 6.18 V emu^{-1}. The measurement was performed while the sample is warming at an average rate of approximately 2 K min^{-1}. The temperature dependence of the magnetic susceptibility, χ, exhibited a Curie–Weiss behaviour for the three samples. A good fit of the observed susceptibilities to $1/\chi=(1/C)T-\theta/C$ was obtained (Fig. 3). The best fit (least squares) values of C and θ obtained for the three samples are listed in Table 2. The corresponding effective magnetic moment, p, of the Cu ion was calculated (Table 2) using $p=\sqrt{8}\times C$ [20].

3. Discussion of results

The X-ray patterns of the deuterided samples (Fig. 1), show no lines other than those of Y_2BaCuO_5. From this result we conclude that the deuterium is taken up

TABLE 2. The magnetic parameters which best fit (least squares) the observed (Fig. 3) temperature dependence of the magnetic susceptibilities of the three samples of $D_uY_2BaCuO_5$ with $u=0.00$, 0.61, and 1.31

Deuterium content u	Sample weight (mg)	Curie–Weiss constant C (K emu gr atom^{-1})	Param. Curie temperature θ (K)	Eff. param. moment P (μ_B)
0.00	150	0.462	−52.7	1.92
0.61	183	0.468	−105.3	1.93
1.31	162	0.420	−125.7	1.83

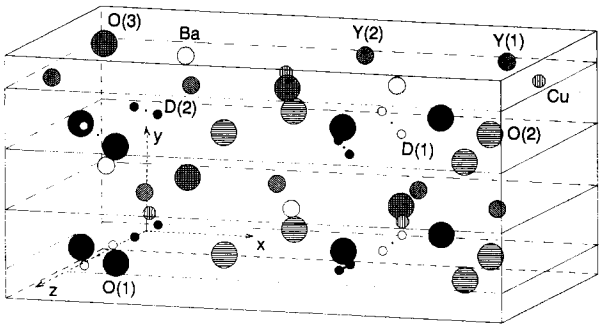

Fig. 4. The proposed crystallographic structure of the deuterated oxide $D_uY_2BaCuO_5$ ($u=0.61$, 1.31). The deuterium sites are only partially occupied. The "green phase" oxide structure remains essentially unchanged upon deuteration.

by the oxide without phase change, hence, forming a solid solution phase. Furthermore, changes in the integrated intensities upon deuteriding are very small, indicating that no major shifts in the heavy atoms (Cu, Ba, Y) positions, takes place upon deuteriding.

Our analysis of the neutron diffraction patterns shows that the deuterium partially occupies two different general positions sites (Table 1) near the inversion centers 1/2 0 0 and 0 1/2 0 (Figs. 4 and 5). In this partial occupancy the D atoms are basically (see below) distributed at random over the positions of each site. It is not possible to tell from our data whether this random occupancy is of single atoms or in pairs with respect to the inversion centers. The intra-pair D–D distances are 0.82 and 0.67 Å (Fig. 5) for the D(1) and D(2) sites, respectively. These distances are unusually small as compared to 1.7–2.1 Å generally found [16] in ternary metal hydrides. Full occupancy of singles and pairs will lead to $u_{max}=2$ and 4 respectively. On the other hand, it was reported [13] that in the process of hydriding, a second phase appears at $u\approx 2$. This fact strongly supports the single occupancies near the inversion centers.

The increase in line width with deuteriding is probably due to breaking up the grains to small crystallites in the process of deuteriding. This process at its extreme

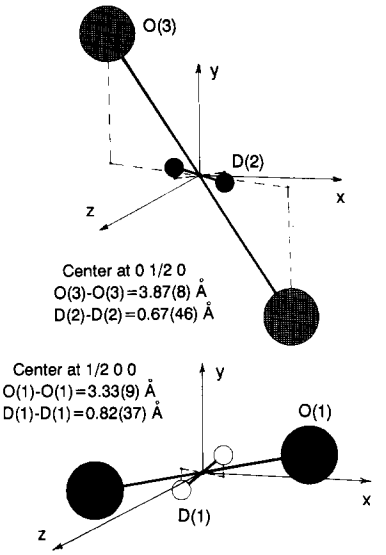

Fig. 5. Blow-ups of the deuterium sites with the neighboring oxygens. The D(2) and O(3) pairs with inversion at 4a (top), and the D(1) and O(1) pairs with inversion at 4b (bottom).

will cause some amorphisation which is responsible for the increase in background upon deuteriding. The hump in the region of $2\theta\approx 50$–$90°$ of the background, is most likely due to short range order (correlation) on the partially occupied deuterium sites. Many metal hydrides exhibit line broadening, increase in background, and background humps [16].

The initial fractional molar volume is (Table 1) practically zero, as compared with 2.9 Å (H atom)$^{-1}$ characteristic of the metal hydrides [16]. Near each inversion center, there is a single oxygen pair (O(1) near 4b and O(3) near 4a, see Fig. 5). On the perpendicular bisector of the line connecting the oxygens of the pair, there are sites with spherical hole size in excess of 0.7 Å^3, available for hydrogen. These holes are large compared to holes of 0.4–0.5 Å^3 available to hydrogen in may metal hydrides [21]. We attribute the difference in the fractional molar volumes between the green phase hydride and the metal hydrides to the hole size available for the hydrogen.

The values of the paramagnetic constants C and θ for the green phase, deduced (Table 2) from the temperature dependence of the magnetic susceptibility (Fig. 3) are in good agreement with values published previously [9]. The negative value of θ indicates that the magnetic interaction is antiferromagnetic. It was found [9–12] indeed, that the green phase undergoes a paramagnetic to antiferromagnetic transition at $T_N\approx 13$–15 K. The decrease of θ upon deuteriding (Table 2) corresponds (within mean field theories) to an increase in the strength of the magnetic interaction [20]. Hence, on the basis of this result, it can safely be predicted that T_N will increase with deuteriding. (Unfortunately, due to technical difficulties, we were

unable to measure the susceptibility at $T<80$ K. We were therefore unable to observe the actual paramagnetic to antiferromagnetic transitions.) The effective magnetic moment deduced for the green phase is 1.92 μ_B, equal to the published [9] value for this compound, and slightly lower than the value of 1.98 μ_B published [22] for the related compound $Y_2Cu_2O_5$. It corresponds to the Cu^{++} (d^9 and $S=1/2$) oxidation state with $g=2.22$.

The change of colour upon hydriding, was at first attributed to a change of the oxidation state of the copper. The room temperature EPR spectra of several hydrides of the green phase were studied [23]. Since no changes in the spectra were found between the nondeuterided and the deuterided compounds, it was concluded that the oxidation state of the Cu^{++} ion does not change through the deuteriding process. The effective magnetic moments deduced from our measurements (Table 2), do not show significant changes upon deuteriding. This result corroborates the conclusion that the copper oxidation state does not change throughout the deuteriding.

4. Conclusion

Hydrogen forms with the green phase a compound with the chemical formula $H_uY_2BaCuO_5$. This compound is a solid solution phase in the concentration range $0<u<2$, and its structure belongs to the space-group *Pnma*. Our neutron diffraction study of deuterided samples shows that D occupies two non-equivalent sites near the inversion centers of the structure. These sites are randomly occupied with a single D per inversion center, leading to $u=2$ at full occupancy (with a single D per inversion center).

It is found, that hole sizes available for the hydrogen atoms are large compared to those in the metal hydrides. This difference explains the small fractional molar volume of the green phase hydride compared to the metal hydrides.

The temperature dependence of the magnetic susceptibility of the green phase and its hydrides, obeys the Curie–Weiss law. The magnitude of the effective magnetic moment (calculated from the Curie constant) corresponds to the Cu^{++} oxidation state and does not vary upon hydriding. The paramagnetic Curie temperature, θ, was found to decrease with hydriding, indicating an increase in the Neel temperature (it was reported that $T_N \approx 13$–15 K for the green phase) with hydriding.

Acknowledgment

JRJ and JRR wish to acknowledge the support of the US Department of Energy, Division of Chemical Sciences, Office of Basic Energy Sciences, under Contract DE-AC02-76CH00016.

References

1 C. Michel and B. Raveau, *J. Solid State Chem., 43* (1982) 73.
2 R. J. Cava, B. Batlogg, R. B. van Dover, D. W. Murphy, S. Sunshine, T. Siegrist, J. P. Remeika, E. A. Reitman, S. Zahurak and G. P. Espinosa, *Phys. Rev. Lett., 58* (1987) 1676.
3 R. Jones, R. Janes, R. Armstrong, N. C. Pyper, P. P. Edwards, D. J. Keeble and M. R. Harrison, *J. Chem. Soc. Faraday Trans., 86* (1990) 676.
4 W. Wong-Ng, H. F. McMurdie, B. Paretzkin, Y. Zhang, K. L. Davis, C. R. Hubbard, A. L. Dragoo and J. M. Stewart, *Powder Diffraction, 2* (1987) 117.
5 R. M. Hazen, L. W. Finger, R. J. Angel, C. T. Prewitt, N. L. Ross, H. K. Mao, C. G. Hadidacos, P. H. Hor, R. L. Meng and C. W. Chu, *Phys. Rev. B, 35* (1987) 7238.
6 Shiyou Pei, A. P. Paulikas, B. W. Veal and J. D. Jorgensen, *Acta Crystallogr. C 46* (1990) 1986.
7 T. Hahn (ed.), *International Tables for Crystallography,* Vol. A, D. Reidel, 1983, p. 288.
8 W. R. McKinnon, J. R. Morton, K. F. Preston and L. S. Selwyn, *Solid State Commun., 65* (1988) 855.
9 K. Kanoda, T. Takahashi, T. Kawagoe, T. Mizoguchi, S. Kagoshima and M. Hasumi, *Jpn. J. Appl. Phys., 26* (1987) L2018.
10 A. Weidinger, J. I. Budnick, B. Chamberland, A. Golnik, C. Niedermayer, E. Recknagel, M. Rossmanith and De Ping Yang, *Physica C, 153–155* (1988) 168.
11 Y. Gross, F. Hartmann-Boutron, J. Odin, A. Berton, P. Strobel and C. Meyer, *J. Magn. Magn. Mater., 104–107* (1992) 621.
12 R. Buriel, M. Castro, C. Pique, A. Salinas-Sanchez and R. Saez-Puche, *J. Magn. Magn. Mater., 104–107* (1992) 627.
13 J. R. Johnson, J. J. Reilly, Z. Gavra and X. Q. Yang, *J. Less-Common Met., 172–174* (1991) 433.
14 J. J. Reilly, M. Suenga, J. R. Johnson, P. Thompson and A. R. Moodenbaugh, *Phys. Rev. B, 36* (1987) 5694.
15 H. Peisl, in G. Alefeld and J. Volkl (eds.), *Hydrogen in Metals I, Topics in Applied Physics,* Vol. 28, Springer, Berlin, 1978, pp. 53–74.
16 K. Yvon and P. Fischer, in L. Schlapbach (ed.), *Hydrogen in Intermetallic Compounds I,* Springer, Berlin, 1988, pp. 87–138.
17 D. B. Wiles and R. A. Young, *J. Appl. Crystallogr., 14* (1981) 149.
18 H. M. Rietveld, *J. Appl. Crystallogr., 2* (1969) 65.
19 D. B. Wiles, *Program for Rietveld Analysis of X-ray and Neutron Powder Diffraction Patterns*, DBW 3.2, 4 May 1982, unpublished work.
20 J. S. Smart, *Effective Field Theories of Magnetism,* W. C. Saunders, 1966, pp. 8.
21 D. G. Westlake, *J. Less-Common Met., 91* (1983) 1.
22 R. Troc, Z. Bukowski, R. Horyn and J. Klamut, *Phys. Lett., 125* (1987) 222.
23 Z. Gavra, *EPR Study of Green Phase Hydrides,* unpublished work, 1989.